Egyptian Journal of
Forensic Sciences

ORIGINAL ARTICLE

Open Access

Tert-butylhydroquinone prevents cyclophosphamide induce lung toxicity in rats via inhibiting oxidative stress and apoptosis: in vivo and in silico study

Mahrous A. Ibrahim[1,2]*, Ayman Fathi Elsharawy[3,4], Waleed E. Abo Baraka[5,6], Athar M. Khalifa[7], Metwally E Abdalla[2], Mohamed S. Nafie[8], Shaimaa A. Shehata[2] and Gamal Abdelrahman Bakhaat[9,10]

Abstract

Background Cyclophosphamide (CP) is a chemotherapeutic and immunosuppressive agent that induces oxidative stress, causing lung tissue damage.

Aim The study aims to explore the antioxidant role of tert-butylhydroquinone (TBHQ) in ameliorating CP-induced lung toxicity exhibited as oxidative stress and programmed cell death.

Methods Thirty-two adult male rats were allocated randomly into four groups: group 1 (control), group 2 TBHQ 50 mg/kg orally for 14 days, and group 3 single dose of (200 mg/kg, CP, i.p.) on the 9th day. In group 4, TBHQ (50 mg/kg, orally) was provided for 14 days, and (200 mg/kg, CP, i.p.) was administrated on the 9th day. Rats' body and lung weight were measured. Oxidative stress marker malondialdehyde (MDA) and pulmonary tissue enzymatic antioxidant levels were assessed: glutathione S transferase, catalase, superoxide dismutase, and glutathione peroxidase. Additionally, glutathione level was measured. Assessment of the levels of TNF-α, IL-1β, and IL-6 were done as well as histopathological and immunohistochemistry investigations. Molecular docking studies of the protein structures of p53-MDM2, IL-6, and IL-1β were performed.

Results CP-intoxicated rats demonstrated a significant decline (CAT, GPx, SOD, GST, and GSH) levels and a significant increase in MDA levels. The proinflammatory parameters (TNF-α, IL-6, IL-1ß) were significantly elevated in group 3. The noted biochemical changes, accompanied by histopathological destruction, indicate CP-induced pulmonary tissue injury. TBHQ played a protective role by attenuating most of the aforementioned biochemical alterations and histopathological distortions in rats' lungs.

Conclusions TBHQ might be utilized as a potential ameliorative agent to inhibit CP-induced pulmonary toxicity via TBHQ's antioxidant and anti-inflammatory effects.

Keywords Tert-butylhydroquinone, Cyclophosphamide, Apoptosis, Molecular docking, Toxicity, Lung

---

*Correspondence:
Mahrous A. Ibrahim
mabdulbaset@ju.edu.sa; mahrous.ibrahim@med.suez.edu.eg
Full list of author information is available at the end of the article

Background

Cytotoxic drugs are known to damage different tissues following systemic administration. Pulmonary toxicity caused by antineoplastic agents is a significant cause of respiratory failure (Kanno et al. 2009; Vahid and Marik 2008). Cyclophosphamide (CP) is a potent chemotherapeutic and immunosuppressive agent widely used to treat a variety of serious health conditions (de Jonge et al. 2005). Cyclophosphamide has proven to be associated with various toxicities (Ayza et al. 2022; Emadi et al. 2009), including nephrotoxicity (Salama et al. 2022), gonadal toxicity (Kim and Chan 2017), hepatotoxicity (Devi and Mazumder 2016), teratogenicity, cardiotoxicity, and pulmonary toxicity (Said et al. 2016). CP known as an alkylating agent of nitrogen mustard was first synthesized by Arnold et al. in 1958 (Arnold et al. 1958; Ayza et al. 2022). CP is considered a prodrug, and cytochrome-P450 is needed for metabolic activation (Kachel and Martin 1994; de Jonge et al. 2005).

The hydroxylation of CP by P450 enzymes results in 2 4-hydroxycyclophosphamide (OHCP) and 3 aldophosphamide (ALDO). OHCP is converted by enzymatic oxidation into the non-cytotoxic 4-ketocyclophosphamide (KCP). While ALDO is detoxified by aldehyde dehydrogenases into the cytotoxically inactive carboxyphosphamide (CARB) and to acrolein by bicarbonate ions (Voelcker 2020). The main active metabolites of CP are phosphoramide mustard, acrolein, and chloroacetaldehyde (Mills et al. 2019). Resultant phosphoramide mustard possesses cytotoxic activity through its effect on deoxyribonucleic acid (DNA), while acrolein is considered a toxic metabolite responsible for CP toxicity (Sun et al. 2014). Although significant lung injury is linked to CP toxicity, the pathogenesis of CP-induced lung damage remains unclear (Saghir et al. 2020; Vahid and Marik 2008). Lung injury could be attributed to direct injury to pneumocytes that leads to the release of pro-inflammatory cytokines, generation of reactive oxygen species (ROS), and the initiation of the inflammatory pathways (Conte et al. 2022; Vahid and Marik 2008). CP causes lung injury in rats by reducing the antioxidant enzymes, such as superoxide dismutase (SOD), glutathione peroxidase (GPx), catalase (CAT), and glutathione S transferase (GST). Moreover, CP depletes glutathione (GSH) as a protective antioxidant (Mombeini et al. 2022). Simultaneously, tumor necrosis factor-α (TNF-α), Interleukin-6 (IL-6), interleukin-1β (IL-1β), and malondialdehyde (MDA) raised by CP in rats' lung tissue (Jiang et al. 2017; Mombeini et al. 2022; Saghir et al. 2020).

Recently, available antioxidants have shown a protective influence against CP-induced lung injury via inhibition of oxidative stress induced by chemotherapy (Alsemeh and Abdullah 2022; Ayza et al. 2022; Patra et al. 2012; Saghir et al. 2020). Tert-butylhydroquinone (TBHQ) is a synthetic soluble phenolic antioxidant compound used as a food additive, cosmetic products, and pharmaceutical products (Duan et al. 2016). TBHQ with the molecular formula of ($C_{10}H_{14}O_2$) is a metabolite of butylated hydroxyanisole, a widely used compound at approved concentrations in food to reduce or inhibit oxidation reactions (Khezerlou et al. 2022).

TBHQ, the synthesized phenolic antioxidant, protects proteins and DNA from oxidative stress damage (Deng et al. 2021, p. 2). It plays a main role in nuclear factor erythroid 2-related factor 2 (Nrf2) signaling pathway activation in several types of cells and tissues (Boss et al. 2018; Meng et al. 2020). Notably, Nrf2 is a transcription agent that acts as a sensor for oxidative stress (Koh et al. 2009). Nrf2 accumulates in the cytoplasm and travels to the nucleus to mediate cytoprotective gene expression through antioxidant-responsive elements (AREs) (Kensler et al. 2007; Xu et al. 2017). Thus, TBHQ results in increased gene expression of SOD, glutathione, and CAT (Pérez-Rojas et al. 2011). Additionally, Nrf2 withstands oxidative stress by suppressing or preventing NADPH oxidase from being expressed (Zhao et al. 2020).

It has been proved that TBHQ has antioxidative effects via mitigating ROS synthesis which is involved in several diseases through different cellular mechanisms (Aldaba-Muruato et al. 2024; Wu et al. 2015). Moreover, TBHQ alleviated apoptosis and lipid peroxidation in oxidative stress conditions (R. Li et al. 2020; López et al. 2022).

According to previous studies, TBHQ reduces the production of inflammatory cytokines like TNF-α, IL-6, IL-1β, and ROS (R. Li et al. 2020; Z.-W. Zhang et al. 2020). Various experimental animal research supported the TBHQ protective antioxidant effect in different organs and diseases, such as ischemia/reperfusion injury in the liver and kidney (Zeng et al. 2017), traumatic brain injury (Saykally et al. 2012), hypoxic-ischemic brain damage (J. Zhang et al. 2018), Alzheimer's disease (Akhter et al. 2011), nephrotoxicity (Pérez-Rojas et al. 2011), and scrotal heat-induced oxidative stress (Y. Li et al. 2014). Despite the beneficial effects of TBHQ observed in previous experimental studies of several illnesses, some potential limitations were present. Firstly, the outcomes could not accurately reflect the therapeutic impact on the individuals. Most of these studies examined the potential therapeutic effect of TBHQ on a rat model for a short period of time, which may not be enough to prove the effect (Yang et al. 2023). In addition, TBHQ's effects in the disease setting were different based on distinct organ sensitivities to TBHQ, TBHQ concentrations, and its optimal dose (Zhu et al. 2022). We postulate that TBHQ could induce a robust defensive impact on rats' lung toxicity induced by CP. The present study was prepared to

explore the possible protective mechanisms of TBHQ to inhibit CP toxicity such as oxidative stress, apoptosis, and lung insult in rats, and to take knowledge of the subject a step further.

Aims of the study

The current study was done to determine the biochemical and histopathological changes in CP-induced pulmonary toxicity in rats and to study the potential protective effect of TBHQ on inhibiting CP toxicity.

Methods

Drugs and chemicals

Cyclophosphamide (Endoxan®) 1 g vial (Baxter Oncology GmbH, Germany) was administered as one dose (200 mg/kg; i.p.) on day 9 to induce acute lung toxicity. It was freshly dissolved in 10 mL of normal saline (0.9%) for use (Alsemeh and Abdullah 2022). Tert-butylhydroquinone (99% purity) was purchased from Sigma-Aldrich as a white crystalline fine powder and stored in a closed container in a cool, dry place when not in use. TBHQ dose was prepared by dissolving 100 mg of TBHQ in 100 μL of dimethylsulfoxide (DMSO, Sigma-Aldrich, Saint Louis, MO, USA) and then diluted with buffered sterile phosphate saline (PBS, pH 7.4), steadily stirring in the absence of light until the desired concentration of 5 mg/mL TBHQ in 1% DMSO was delivered immediately (Aldaba-Muruato et al. 2024). Diagnostic kits and chemicals used in the experiment were obtained from Sigma Chemical Company, St. Louis, USA, and Bio Diagnostics Co., (Giza, Egypt).

Animals

Thirty-two adult male 8-week-old albino rats, weighing 200–230 g were purchased from Helwan Breeding Centre, Egypt. Prior to the study, the animals were acclimatized for 1 week in small polycarbonate cages (five rats/cage) under standard pathogen-free conditions and quite a non-stressful special room. Animals were freely given access to a standard commercial diet (ATMID Company, Egypt) and tap water. A good, ventilated room, lighting (12-h light: 12-h dark) with temperature under control (24 ± 2 °C) with relative humidity (55 ± 5%). Pain, distress, and suffering were kept to a minimum grade. Animals were anesthetized before blood sample collection and before scarification. Scarification of the animals was done in an appropriate manner. The initial rats' body weight was recorded before starting the experiment and administrating the drugs. The experiment and its procedures complied with the Guide of the Faculty of Science, Suez Canal University research ethics committee of Animal Care and Use (approval no: REC129/2022) and were performed according to the Care and Use of Laboratory Animals published by the US National Institutes of Health (NIH Publication No. 85–23, revised 2011).

Experimental design

The rats were distributed randomly into 4 groups ($n = 8$/group) as following (Scheme 1):

> *Group 1 (control group):* rats received 1% DMSO (vehicle for TBHQ) orally for 14 days and a single dose of normal saline by intraperitoneal (i.p) routes on the 9th day of the study.
> *Group 2 (TBHQ):* rats received TBHQ 50 mg/kg b.w. in 1% DMSO orally for 14 days and normal saline i.p on day 9th (Nna et al. 2020).
> *Group 3 (CP):* rats received 1% DMSO orally for 14 days and a single 200 mg/kg b.w dose of CP i.p on the 9th day of the treatment schedule to induce acute lung toxicity (Alsemeh and Abdullah 2022).
> *Group 4 (CP + TBHQ):* rats received TBHQ as in group 2, and CP on day 9 as in group 3.

The single dose of CP (200 mg/kg, i.p.) used in this study was confirmed to induce oxidative stress and pulmonary toxicity in rats (Habibi et al. 2020; Saghir et al. 2020; Shokrzadeh et al. 2015). The selection of a dose of 50 mg/kg b.w. had no negative effects on different biological indices such as liver enzymes, TNF-α and IL-1β and semen parameters (Liu et al. 2022; Nna et al. 2020; H. Zhang et al. 2021). Moreover, The dose of TBHQ used in the current study has been identified to activate cytoprotective genes in rat models of oxidative injury in many studies (Nna et al. 2020; Ujah et al. 2021; Zeng et al. 2017).

Sample preparation

Twenty-four hours after the last dose, ketamine/xylazine (50/5 mg/kg, i.p) was administered to anesthetize the animals (Alsemeh and Abdullah 2022). After fasting overnight, rats were euthanized by cervical dislocation. To eschew any potential diurnal variations in the level of the antioxidant enzyme, the rats were sacrificed between 8:00 and 10:00.

Before scarification of the rats, the required blood samples were gathered from the retro-orbital sinus. All blood samples were centrifuged at 4000 rpm and 4 °C for 10 min to obtain clear homogenates supernatant. The supernatants were stored frozen at -80 °C. To get the lungs cleaned from red blood cells and clots, after sacrifice, the lungs were removed and washed with cold phosphate-buffered saline (pH 7.4 containing 0.16 mg/mL heparin). Left lung tissue was homogenized for 3 min in 1:10 volumes of ice-cold potassium phosphate buffer (50 mM; pH 7.5) on ice (Teflon-glass homogenizer).

Ibrahim *et al. Egyptian Journal of Forensic Sciences*   (2024) 14:20

Page 4 of 15
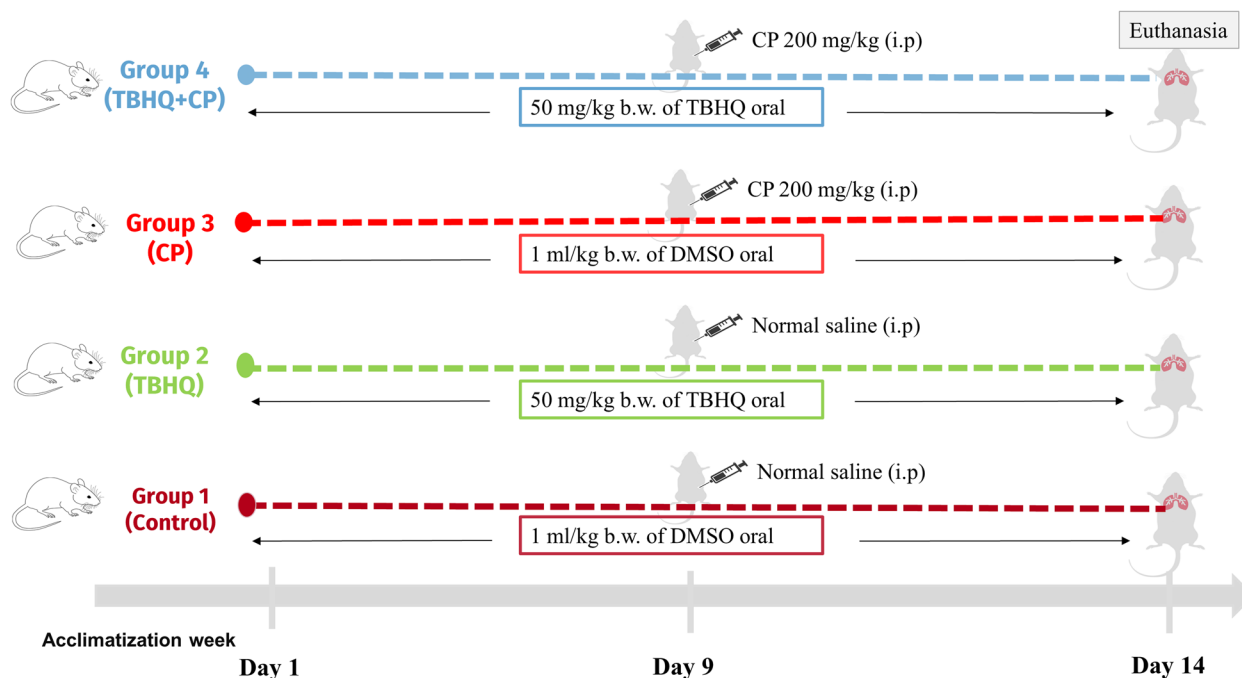
Scheme 1 Experimental timeline. Dimethyl sulfoxide (DMSO); tert-butylhydroquinone (TBHQ); cyclophosphamide (CP); intraperitoneal (i.p)

Body weight, lung weight, and the lung/body weight ratio measurement

At the beginning of the experiment, Initial body weight (IBW) and final body weight (FBW) at the end of the study were assessed for each rat. Lung weight (LW) was measured after removing and washing them with normal saline. Relative body weight (RBW) and relative lung weight (RLW) were calculated based on these equations: RBW = (final body weight / initial body weight) × 100 and RLW = (lung weight/final body weight) × 100.

Antioxidant enzymes and oxidative stress biomarkers analysis

The SOD activity was determined using the Sun et al. technique (Sun et al. 1988), while the assessment of CAT activity was done based on Aebi method (Aebi 1984). In addition, the Lawrence and Burk method was adopted to calculate GPx activity (Lawrence and Burk 1978). The previous enzymes were expressed as units (U)/g of protein. The GST enzyme activity level was assessed according to the Habig and Jacoby method (Habig and Jakoby 1981). The GSH level was determined using the method described by Sedlak and Lindsay (Sedlak and Lindsay 1968), while the MDA level was determined in tissue homogenate according to the Placer method (Placer et al. 1966). Both MDA and GSH levels were mentioned in terms of nmol/g of tissue.

Assessment of the TNF-α, IL-1β, and IL-6 proinflammatory cytokines levels

TNF-α, IL-1, and IL-6 pro-inflammatory cytokines were quantified in tissue homogenates using commercial rat ELISA kits.

Histopathological assessment

A 10% neutral buffered formalin solution was used to fix lung tissue samples for 48 h. Then, gradual ascending ethyl alcohol (from 70% to absolute) was used to dehydrate the samples. Next, they were cleared in xylene, followed by paraffin embedding. The paraffin blocks were sliced into 5-μm-thick sections using a Leica RM 2155 microtone (Leica Biosystems, Buffalo Grove, IL, USA). These sections were then processed and stained using H&E (hematoxylin and eosin) dyes. To determine the severity of the lung injury, a blinded pathologist examined the H&E slides under a light microscope. Defined parameters were observed to evaluate the lung damage. The parameters include edema, hemorrhage, and/or congested alveolar capillaries, alveolar septal thickening, inflammatory cell infiltration, and tissue involvement. Blinding assessment was ensured during histopathological evaluation to minimize bias in subjective assessments.

Immunohistochemistry evaluation of p53 and Bcl-2

The lung sections were prepared as described above, but positively charged slides were used. Immunohistochemistry

was performed in accordance with SABC instructions and SABC kits. Briefly, slides were treated with 3% H_2O_2 and 5% bovine serum albumin (BSA) blockage for antigen retrieval, then incubated with primary antibodies, tumor suppressor p53, and B-cell lymphoma-2 (Bcl-2) overnight at 4 ℃. Horseradish peroxidase (HRP)-conjugated secondary antibody was used at a 1:700 in blocking solution for 1 h at 37 ℃. 3,3-Diaminobenzidine tetrahydrochloride (DAB), which was used as chromogen, and hematoxylin (Vector, Houston, TX, USA), was used as a counter stain for the nuclei.

Molecular docking
Protein structures of p53-MDM2 protein (PDB = 1YCR), IL-6 (1ALU), and IL-1β (PDB = 1ITB) were freely adopted from the protein Data Bank (https://www.rcsb.org/structure/). The ligand structure of THBQ was retrieved from PubChem (PubChem, n.d.). The protein structure was optimized by adjusting the amino acids with missing atoms or alternative positions, and ligand structures were built, optimized, and energetically favored using Maestro. The Auto-Dock Vina software was used to conduct the molecular docking study following the routine work of Nafie et al. (Nafie et al. 2019) of defining the grid box dimensions box of 10 Å in the *x*, *y*, and *z* directions cantered on the ligand. Docking results were interpreted in terms of binding energy and ligand-receptor interactions. Chimera-UCSF was used to analyze the binding disposition and interactive analysis.

Statistical analysis
Statistical Package for the Social Sciences (SPSS) software, version 23 for Windows (SPSS, Inc., Chicago, IL, USA), was used to analyze our data (SPSS, 2015). Numerical data were presented as mean ± standard deviation (SD). Each group of rats was declared in the table or figure legends. Once obtaining the homogeneity of variance between treatment groups by Bartlett's test and analyzing mean differences between experimental groups for each parameter separately, a one-way analysis of variance (ANOVA) followed by Student-Newman-Kaul's test was conducted. Values of $p < 0.05$ were statistically significant.

Results
Effect of TBHQ and CP on body weight, lung weight, and the lung/body weight ratio
The effects of TBHQ, CP, and the combination of TBHQ with CP on animal IBW, FBW, RBW, LW, and RLW are shown in (Table 1). It was shown that both FBW and RBW were significantly decreased in group 3 (CP) in comparison with group 1 ($p < 0.05$). Coadministration of TBHQ with CP (group 4), significantly increased both FBW and RBW compared to group 3. There was a significant rise in LW and RLW among group 3 compared to group 1 ($p < 0.05$). Coadministration of TBHQ with CP in group 4 significantly decreased LW and RLW compared to group 3 ($p < 0.05$).

Effect of TBHQ and CP on antioxidant enzymes activity and oxidative stress biomarker levels
The antioxidant enzyme levels (CAT, SOD, GST, and GPx), GSH, and MDA showed a non-significant difference ($p ˃ 0.05$) in group 2 (TBHQ) compared with control group 1. In contrast, in CP-intoxicated rats (group 3), there was a statistically significant decrease in antioxidant enzyme activities and an increase in the level of MDA ($p < 0.05$) when compared with control groups. Coadministration of TBHQ with CP-intoxicated rats (group 4) exhibited a statistically significant improvement in antioxidant enzyme status and reduction of MDA level (Table 2).

Table 1 Effects of cyclophosphamide (CP), tert-butylhydroquinone (TBHQ), and their combination on body weight gain, lung weights of rats' groups, after 2 weeks of treatment

Parameters	Group 1 (control)	Group 2 (TBHQ)	Group 3 (CP)	Group 4 CP + TBHQ
IBW (g)	202.50 ± 5.45	205.83 ± 3.82	203.83 ± 2.99	202.17 ± 4.58
FBW (g)	220.25 ± 4.98	222.67 ± 3.98	191.50 ± 2.98[ab]	214.50 ± 5.54[c]
RBW	108.58 ± 1.35	108.18 ± 0.37	94.36 ± 1.03[ab]	106.10 ± 1.26[c]
LW(g)	2.51 ± 0.12	2.67 ± 0.08	3.81 ± 0.12[ab]	2.62 ± 0.08[c]
RLW	1.13 ± 0.07	1.20 ± 0.05	2.00 ± 0.07[ab]	1.22 ± 0.03[c]

Data are mean ± SD. (*n* = 8 rats/group). *TBHQ* tert-butylhydroquinone, *CP* cyclophosphamide, *IBW* initial body weight, *FBW* final body weight, *RBW* relative body weight, *LW* lung weight, *RLW* relative lung weight

Relative body weight = (final body weight/initial body weight) × 100

Relative lung weight = (lung weight/body weight) × 100

-Significant at $p < 0.05$ (one-way analysis of variance (ANOVA) followed by Student-Newman-Kaul's test was conducted)

[a] Compared to the control (group 1) group

[b] Compared to TBHQ (group 2)

[c] Compared to CP (group 3)

Ibrahim *et al. Egyptian Journal of Forensic Sciences*   (2024) 14:20

Page 6 of 15

Table 2 Effects of cyclophosphamide (CP), tert-butylhydroquinone (TBHQ), and their combination on oxidative stress markers in the lungs of rats' groups, after 2 weeks of treatment

Parameters	Group 1 (control)	Group 2 (TBHQ)	Group 3 (CP)	Group 4(CP + TBHQ)
CAT	69.75 ± 2.60	70.00 ± 1.69	32.63 ± 2.33[ab]	65.63 ± 2.62[c]
SOD	65.38 ± 2.50	66.13 ± 1.73	35.50 ± 2.45[ab]	62.88 ± 2.17[c]
GPx	284.00 ± 3.93	283.50 ± 4.17	188.63 ± 3.81[ab]	273.50 ± 6.55[c]
GST	45.38 ± 2.92	47.13 ± 4.02	32.3 ± 2.87[ab]	42.00 ± 3.42[c]
GSH	85.63 ± 3.54	86.17 ± 2.56	43.00 ± 3.30[ab]	80.88 ± 3.94[c]
MDA	383.13 ± 5.06	378.83 ± 7.49	464.0 ± 11.10[ab]	362.75 ± 9.91[c]

Data are mean ± SD. ($n = 8$ rats/group). *Group 1* control, *Group 2* TBHQ, *Group 3* CP, *Group 4* CP + TBHQ, *CP* cyclophosphamide, *CAT* catalase, *SOD* superoxide dismutase, *GPx* glutathione peroxidase, *GST* glutathione S transferase, *GSH* Glutathione *MDA* malondialdehyde

-Significant at $p < 0.05$ (one-way analysis of variance (ANOVA) followed by Student-Newman-Kaul's test was conducted)

[a] Compared to the control (group 1) group

[b] Compared to TBHQ (group 2)

[c] Compared to CP (group 3)

Effect of TBHQ and CP on proinflammatory cytokines (TNF-α, IL-6, and IL-1ß) levels

Table 3 shows the proinflammatory cytokines in the control and tested groups. There were no significant differences in the control and TBHQ groups. The (TNF-α, IL-6, and IL-1ß) levels were statistically significantly elevated in CP-intoxicated rats in group 3 (CP) ($p < 0.05$) compared with control group 1. However, coadministration of TBHQ with CP in group 4 significantly decreases the levels of the proinflammatory markers ($p < 0.05$) in comparison to group 3.

Histopathological light microscopic findings in lung

Light microscopy photomicrographs of illustrative histological sections of rat lungs from control and TBHQ groups are shown in Fig. 1. It depicts normal lung histological architecture, involving normal (pneumocytes, airway bronchioles, alveolar septa, and blood vessels) in control and TBHQ groups. On the contrary, group 3 showed interalveolar septum thickening, complete alveolar blockage, and many enlarged blood vessels. The resultant thickening was prominent because of the significant

inflammatory edema mixed with erythrocyte leakage in the interalveolar erythrocytes in the interalveolar septa. In addition to significant inflammatory cell infiltration, lymphocytes, and a few granulocytes. Marked compensatory emphysema combined with thickened septa was observed (Fig. 2A, B). On the other hand, coadministration of TBHQ in CP-intoxicated rats revealed partial obstruction of the alveolar septa, with congested blood vessels that were surrounded by some inflammatory cells (Fig. 2C, D).

Immunohistochemical results

Results of p35 immunostaining study are shown in Fig. 3. Lung tissue slides in the control and TBHQ groups showed negative staining of the nuclei of the alveolar cells (Fig. 3A, B). Strong positive immunostaining for p53 was observed in the nuclei of the alveolar cells of the CP-treated rat group 3 indicating the apoptosis process. Administration of TBHQ in CP intoxicated rats (group 4) inhibiting p53 activity indicating antiapoptotic activity of TBHQ. In Fig. 4, Bcl-2 immunostaining investigation revealed that Bcl-2 was positively expressed with slightly

Table 3 Effects of cyclophosphamide (CP), tert-butylhydroquinone (TBHQ), and their combination on inflammatory markers in the lungs of rats' groups, after 2 weeks of treatment

Parameters	Group 1 (control)	Group 2 (TBHQ)	Group 3 (CP)	Group 4 (CP + TBHQ)
TNF-α	2053.63 ± 28.04	2072.38 ± 39.44	3106.75 ± 84.12[ab]	2353.75 ± 55.01[c]
IL-6	109.38 ± 2.83	110.75 ± 3.06	168.13 ± 3.98[ab]	122.38 ± 5.32[c]
IL-1β	11.45 ± 0.21	11.53 ± 0.28	26.31 ± 0.59[ab]	15.83 ± 1.84[c]

Data are mean ± SD. ($n = 8$ rats/group). *Group 1* control, *Group 2* tert-butylhydroquinone (TBHQ), *Group 3* cyclophosphamide (CP), *Group 4* CP + TBHQ, *TNF-α* tumor necrosis factor-α (pg/g tissue), *IL-6* interleukin 6 (pg/g tissue), *IL-1β* interleukin 1 beta (ng/g tissue)

- Significant at $p < 0.05$ (one-way analysis of variance (ANOVA) followed by Student-Newman-Kaul's test was conducted)

[a] Compared to the control (group 1)

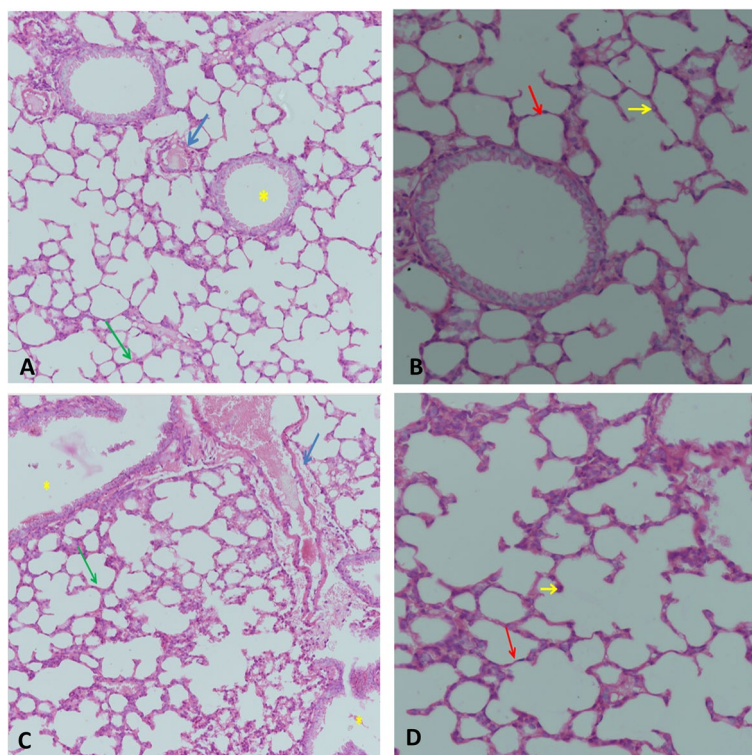[b] Compared to TBHQ (group 2)

[c] Compared to CP (group 3)

Fig. 1 A hematoxylin and eosin stained sections of a rat lung in groups 1 and 2. Group 1 (**A**) H&E-200×stained lung sections in the control group 1 showing normal lung alveoli, interalveolar septum (green arrow), and air bronchioles (yellow star) also the blood vessels appear normal (blue arrow). **B** H&E-400×stained lung sections in group 1 (control) showing normal pneumocytes type I (red arrow) and type II (yellow arrow). Group 2 (**C**) H&E-200×stained lung sections in group 1 showing normal lung alveoli, interalveolar septum (green arrow), and air bronchioles (yellow star). The blood vessels appear normal. (D) H&E-400×stained lung sections in group 1 showing normal pneumocytes type I (red arrow) and type II (yellow arrow)

different intensity and distribution in the lung tissue of both group 1 and group 2 (Fig. 4A, B). Negative staining of Bcl-2 was observed in the CP group 3 (Fig. 4C) while administration of TBHQ in group 4 showed strong Bcl-2 staining (Fig. 4D).

Molecular docking

The MDM2 oncoprotein is a cellular inhibitor of the p53 tumor suppressor in that it can bind the transactivation domain of p53 and downregulate its ability to activate transcription. The IL-6 and IL-1β are pro-inflammatory cytokines, so their inhibition is one of the therapeutic targets for anti-inflammatory functions. Hence, THBQ was screened for binding activity using a molecular docking study toward p53, IL-6, and IL-1β proteins to highlight the virtual mechanism of target protein inhibition.

As seen in Fig. 5A, THBQ was docked inside the p53-binding domain with the binding energy of −12.26 kcal/mol and formed one hydrogen bond with Gln 59 through hydroxyl group (−OH) as a donor with a bond length of 1.83 A.

Additionally, it formed a series of Van der Waals forces with Phe 55, Lys 24, and other lipophilic amino acids inside the pocket. Hence, molecular docking results exhibited that the THBQ may serve as a promising inhibitor to P53 besides its regulator protein MDM2. Hence, the apoptosis pathway of cells will be stopped.

Regarding inhibiting IL-6 and IL-1β proteins, THBQ was docked inside the two proteins with binding energies of −11.65 and −14.32 kcal/mol, respectively. As seen in Fig. 5B, it formed one hydrogen bond with Arg 179 through hydroxyl group (−OH) as an acceptor with a bond length of 1.85 A. Additionally, it formed a series of Van der Waals forces with Arg 182, and other lipophilic amino acids inside the pocket. As seen in Fig. 5C, it formed two hydrogen bonds with Ile 13 and Pro 26 through its two hydroxyl groups as donors with bond lengths of 1.43 and 1.92 A, respectively. Additionally, it formed lipophilic interactions with the lipophilic amino acids inside the pocket. So, based on the molecular docking results, we could conclude the protective role of THBQ as an apoptosis-inhibitor and inflammation-inhibitor.
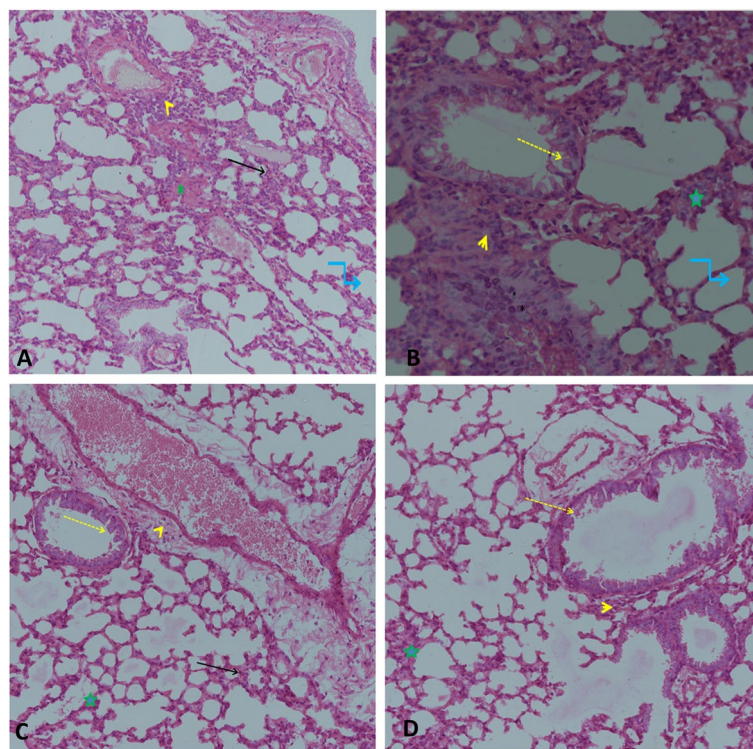
Fig. 2 A hematoxylin and eosin stained sections of a rat lung in groups 3 and 4. **A** H&E-200×stained lung section in CP group 3 showed complete obstruction of the alveoli (black arrow), thickening of interalveolar septae, congested blood vessels, severe edema admixed with extravasated blood (green star) in the interalveolar septa (infiltration of inflammatory cells mainly lymphocytes and few granulocytes (yellow arrowhead) marked compensatory emphysema combined with thickened septa (curved blue arrow). **B** H&E-400×stained lung sections in CP group 3 showing inflammatory cells infiltrated the interalveolar septae of mainly lymphocytes and few granulocytes (yellow arrowhead) epithelium destruction of air bronchioles (yellow dash arrow) with marked compensatory emphysema (curved blue arrow) associated with thickened interalveolar septa (green star). **C** H&E-200×stained lung sections in CP and TBHQ group 4 showing partial obstruction of the alveoli (Black arrow), with some thickening of interalveolar septae (green star), with congested blood vessels that are surrounded with some inflammatory cells (yellow arrowhead). The air bronchiolar epithelium appears normal (Yellow dash arrow). **D** H&E-400×stained lung sections in CP and TBHQ group 4 show some alveoli appear normal and others appear with thickening of their alveolar wall (green star), the air bronchioalveolar epithelium appears slightly distorted and destructed with fluid in bronchiolar lumen (yellow dash arrow) some infiltrated cells are present (yellow arrowhead)

Discussion

Cyclophosphamide has both antineoplastic and immunosuppressive effects that could cause adverse toxic reactions in different organs of humans and animals (Ayna et al. 2020). It is proven that CP induces pulmonary toxicity by enhancing apoptosis, inflammation, and oxidative stress (Alsemeh and Abdullah 2022). As a result, there is a need to develop protective antioxidant agents that can be used in conjunction with chemotherapy to reduce its toxic effects (Ayza et al. 2022). The present study highlights the antioxidant and anti-inflammatory effects of TBHQ on lung tissue to inhibit deterioration in the histological pattern, oxidative stress, and programmed cell death induced by CP in rat's lungs.

In the existing study, CP resulted in a significant decrease in both FBW and RBW, accompanied by a rise in lung weight. The decrease in body weight in group 3 is in agreement with CP administration in many studies

(Attia et al. 2023; Raeeszadeh et al. 2022). This may be attributed to anorexia and this could be explained by has harmful effects of CP on the appetite center in the hypothalamus and gastrointestinal tract (Elgohary et al. 2023; Kamiya et al. 2021). It is suggested that severe tissue damage caused by ROS could lead to weight reduction (Badawi 2022). Increasing the lung weight in group 3 in accordance with other studies that revealed CP administration induced a significant rise in LW and RLW, indicating the presence of pulmonary edema (Ashry et al. 2013; Badawi 2022). This observation could be linked to CP-induced pulmonary edema, inflammation, or increased collagen production, as confirmed by the histological results and increased proinflammatory cytokine levels (El-Kashef 2018). Additionally, the ROS production caused by CP intoxication will enhance the direct destruction of pulmonary vascular endothelial cells (Alsemeh and Abdullah 2022). In the current study,
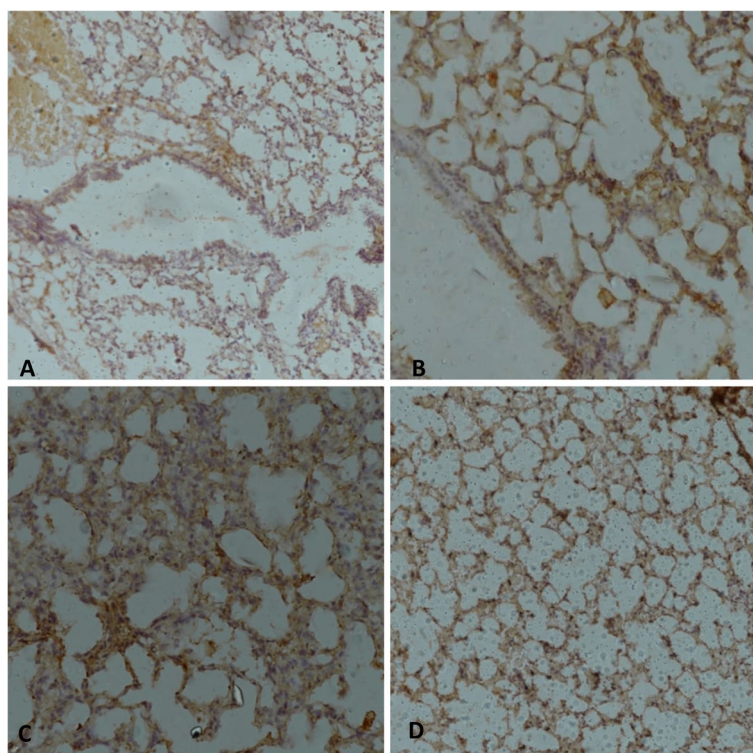
Fig. 3 An p53 immunohistochemistry stained sections of a rat lung in the experimental groups. **A** Group 1 shows negative staining for p53×200 can be observed in the nuclei of the alveolar cells. **B** Group 2 shows negative staining for p53×400 can be observed in the nuclei of the alveolar cells. **C** Group 3 shows strong positive staining for p53×400 can be observed in the nuclei of the alveolar cells. **D** Group 4 shows negative staining for p53×200 can be observed in the nuclei of the alveolar cells

TBHQ restored the rats' FBW and RBW with a decrease of the LW and RLW, which can be a consequence of a protective effect against CP toxicity.

In the current study, CP-induced oxidative stress was exhibited by a reduction of antioxidant enzymes CAT, SOD, GPx, GST, and GSH concentration levels and an increase in lipid peroxidation MDA levels. These findings were in agreement with many studies that observed a decrease in antioxidant enzyme levels accompanied by an increase in MDA levels in the lung following CP intoxication (Alsemeh and Abdullah 2022; Badawi 2022; Ghosh et al. 2015; Şengül et al. 2017). Reduced GSH in the current study was in line with other studies, which revealed a reduction of GSH after the injection of CP in rats (Badawi 2022; El-Kashef 2018; Şengül et al. 2017). El-Kashef, 2017 stated that CP increased MDA levels, causing alterations in the physiological activities of various enzymes, resulting in lower GSH restoration capacity (El-Kashef 2018). GSH as a crucial antioxidant has, a role in cytoprotecting versus oxidative insult (Amiri et al. 2018). Oxidative stress is the end product of an imbalance between oxidants and antioxidants, which results in free radicals generation, which might attach proteins, lipids, and genetic materials of the cells (Chabra et al.

2014; El-Naggar et al. 2015; Omole et al. 2018; Yuan et al. 2014, p. 3). It is proven that GSH is known to be depleted by acrolein (Xiong et al. 2021). The mechanism through which Acrolein induces cellular damage is through generations of free radicals, binding with the GSH and decreasing its level in the cell (Araghi et al. 2018). Meanwhile, CP causes DNA deterioration via an oxidative process and the generation of H_2O_2 (Araghi et al. 2018; El-Naggar et al. 2015). Lipid peroxidation is the main criterion of oxidative stress and MDA is a signal and a marker of lipid peroxidation (Ibrahim et al. 2019). Structural membranes' lipid peroxidation can be induced by free radicals causing interaction with other biomolecules, such as ion pumps, receptors, and enzymes, leading to suppression of their normal actions. The redox balance disruption which is mediated by oxidative stress enhances the alterations of the physiological and biochemical processes, as well as stimulation of many signaling pathways intracellularly, causing upregulation of the synthesis of proinflammatory cytokine and apoptosis induction (Mythili et al. 2004).

In the present study, CP provokes inflammation by increasing the release of proinflammatory cytokines TNF-α, IL-6, and IL-1ß while coadministration of TBHQ with CP has a positive anti-inflammatory effect in group
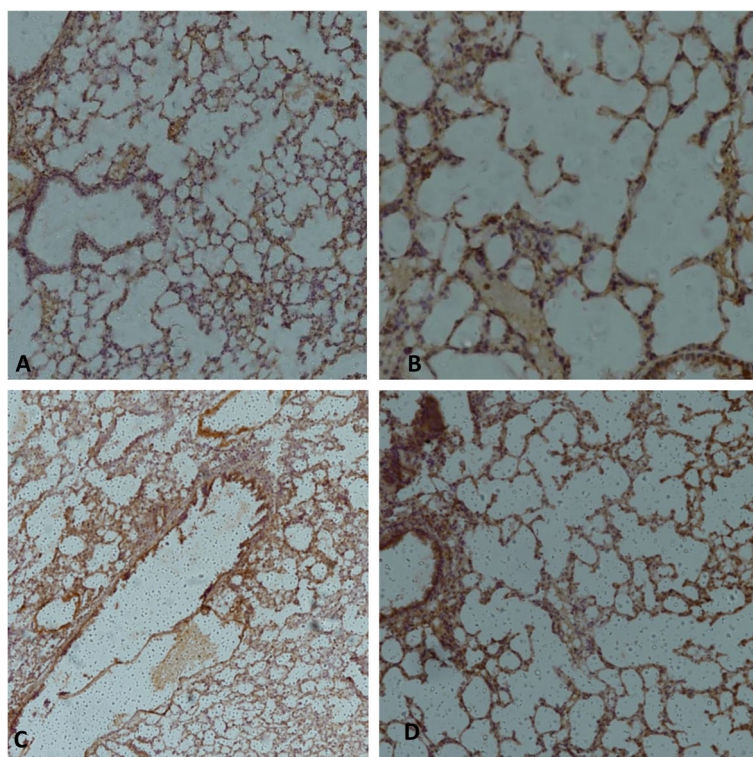
Fig. 4 An Bcl-2 immunohistochemistry stained sections of a rat lung in the experiment groups. **A** Group 1 shows strong staining for Bcl-2×200 can be observed in the nuclei of the alveolar cells. **B** Group 2 shows strong staining for Bcl-2×400 can be observed in the nuclei of the alveolar cells. **C** Group 3 shows negative staining for Bcl-2×200 can be observed in the nuclei of the alveolar cells. **D** Group 4 shows strong staining for Bcl-2×400 can be observed in the nuclei of the alveolar cells

4. These findings were in agreement with other studies (Alsemeh and Abdullah 2022; El-Kashef 2018). Interruption mediated by oxidative stress leads to stimulation of signaling pathways and thus increased synthesis of proinflammatory cytokines (Patra et al. 2012). It is known that TNF-α stimulates an inflammatory cascade, which worsens the tissues' injuries (Möller and Villiger 2006). Additionally, oxidative stress may boost TNF-α synthesis through NF-κβ activation (Imran and Lim 2013).

In the current study, the finding showed that several intracellular signaling pathways were activated by oxidative stress which causes the upregulation of proinflammatory cytokine synthesis (TNF-α, IL-6, and IL-1β). These proinflammatory cytokines were increased in the tissues of CP treated group, which was ameliorated with the cotreatment of TBHQ with CP. The increase in inflammatory reaction with the release of proinflammatory cytokine could be attributed to inflammatory cells such as macrophages, lymphocytes, and neutrophils (Möller and Villiger 2006). These effects are involved in the damage of connective tissue through the proteolytic enzymes release as well as free radicals' release (Ahmed et al. 2015).

TBHQ played a significant role in the amelioration of oxidative stress and inflammatory pathways that were boosted by CP toxicity in group 3. TBHQ is a well-known natural compound that has a dual effect as an antioxidant impact (Sargazi et al. 2015). The generated ROS could be cleared by the system, the enzymes like SOD, CAT, and the reduced GSH, as antioxidant materials (Yuan et al. 2014). In vivo study, TBHQ was able to significantly reduce the biochemical and histological alterations induced by chemicals in tissues other than the lung (Dai et al. 2022; R. Li et al. 2020; Pérez-Rojas et al. 2011). Lilly Veskemaa et al. (2021) found that the administration of TBHQ lessened oxidative stress and improved the survival of ventilator-induced lung damage in mice (Veskemaa et al. 2021).

In the histopathological assessment, group 3 lung tissue showed interalveolar septum thickening, significant inflammatory cell infiltration, edema, complete alveolar blockage, compensatory emphysema, and enlarged blood. The normal lung architecture and immune response were restored by THBQ in group 4 compared with group 3. The results of the current study were consistent with CP toxicity in many studies have
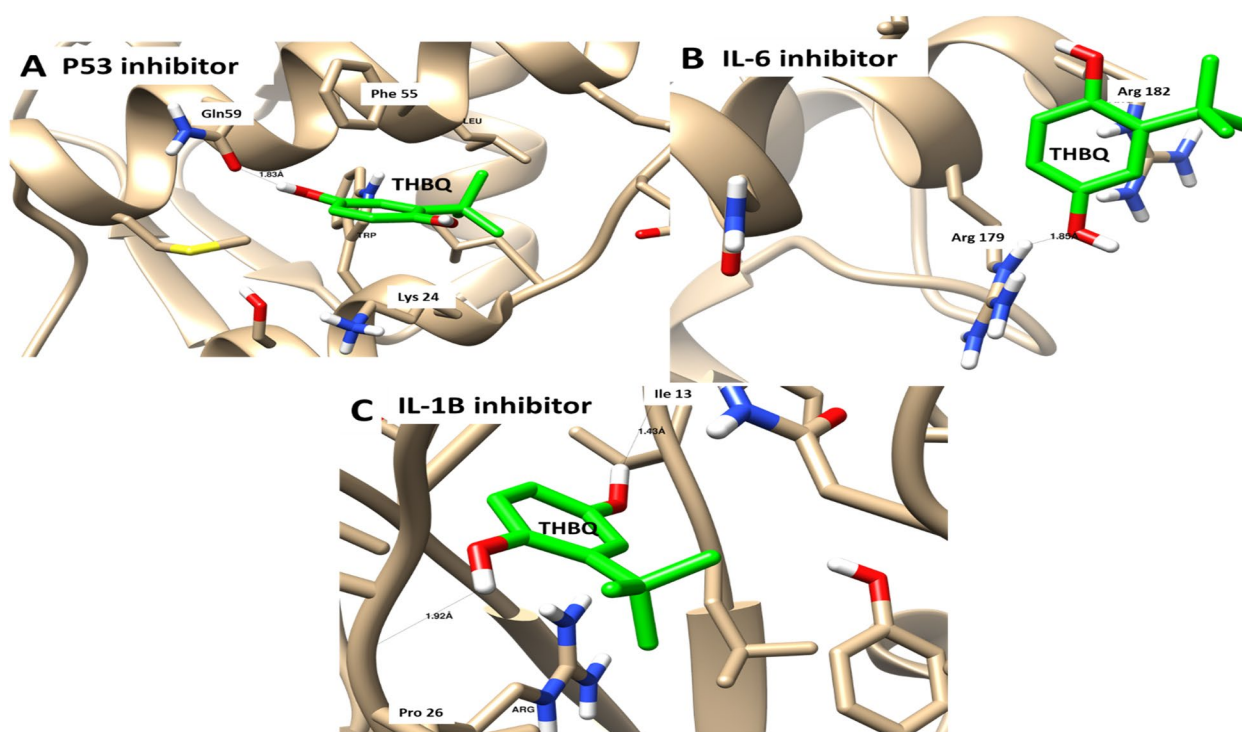
Fig. 5 Molecular docking model/structure showing binding disposition and ligand-receptor interactions of TBHQ (green-colored) inside the binding sites of **A** P53-MDM2 protein as an inhibitor of p53-MDM2 binding. **B** IL-6 protein as an inhibitor of IL-6, and **C** IL-1β protein as an inhibitor of IL-1β. Docking study was performed using AutoDock Vina and three-dimensional images were generated using Chimera-UCSF

stated many histological changes, such as a thickening in the alveolar septa, injuries in the alveolar lumen, alveolar congestion, and lung congestion and cell infiltrations in the pulmonary tissues of the CP-treated group (Badawi 2022; Olama et al. 2018; Şengül et al. 2017). CP treatment prompted inflammatory cell infiltrate which might be explained due to the generation of reactive radicals and release of inflammatory cytokines as mentioned previously. The occurrence of increased numbers of activated neutrophils may be the cause of induced pulmonary injury and pulmonary edema via the excessive elaboration of inflammatory cytokines, proteolytic enzymes, and oxygen radicals (Badawi 2022). Former research findings mentioned that injured alveolar epithelial cells may drive excess generation of mediators and cytokines, which has been associated with histological alterations in the pulmonary parenchyma (Olama et al. 2018). In the same line, previous researchers have identified that CP-treated animals are characterized by markedly increased pulmonary fibrosis which leads to visible fibrous tissue and distortion of lung architecture (Badawi 2022; El-Kashef 2018).

Coadministration of TBHQ in CP-intoxicated rats reverted most of the deleterious histological changes in the lung, depicting the ameliorative role of TBHQ against CP-induced lung damage via decreasing generation of ROS and the lung injury process (Sargazi et al. 2015; Zhao et al. 2020). It was clear from histopathology findings in our study that TBHQ administration attenuates the severity and extent of tissue injury by restraining CP-induced collagen deposition and inflammatory cell infiltration. The study indicated that the protective effect of TBHQ, which has been evidenced in CP-induced pulmonary toxicity in rats by histological studies, is due to its anti-inflammatory and antioxidant properties (Koh et al. 2009; Sargazi et al. 2015). Based on prior research findings, TBHQ has shown several potential therapeutic activities, as well as anti-inflammatory, anticancer, antioxidant, and wound healing properties (Sargazi et al. 2015).

In this study, CP induced the generation of oxidative stress, release of inflammatory cytokines, and alteration in lung architecture while TBHQ decreases the lung injury caused by CP in rats via antioxidant action and free radical-clearing characteristics (Scheme 2).

The molecular docking study highlighted the virtual mechanism of THBQ towards the investigated targets of P53, IL-6, and IL-1β as its molecular target of activity. Based on docking results, THBQ exhibited a good bonding mode of interaction with good binding energy to prove the stability of the drug-target complex.
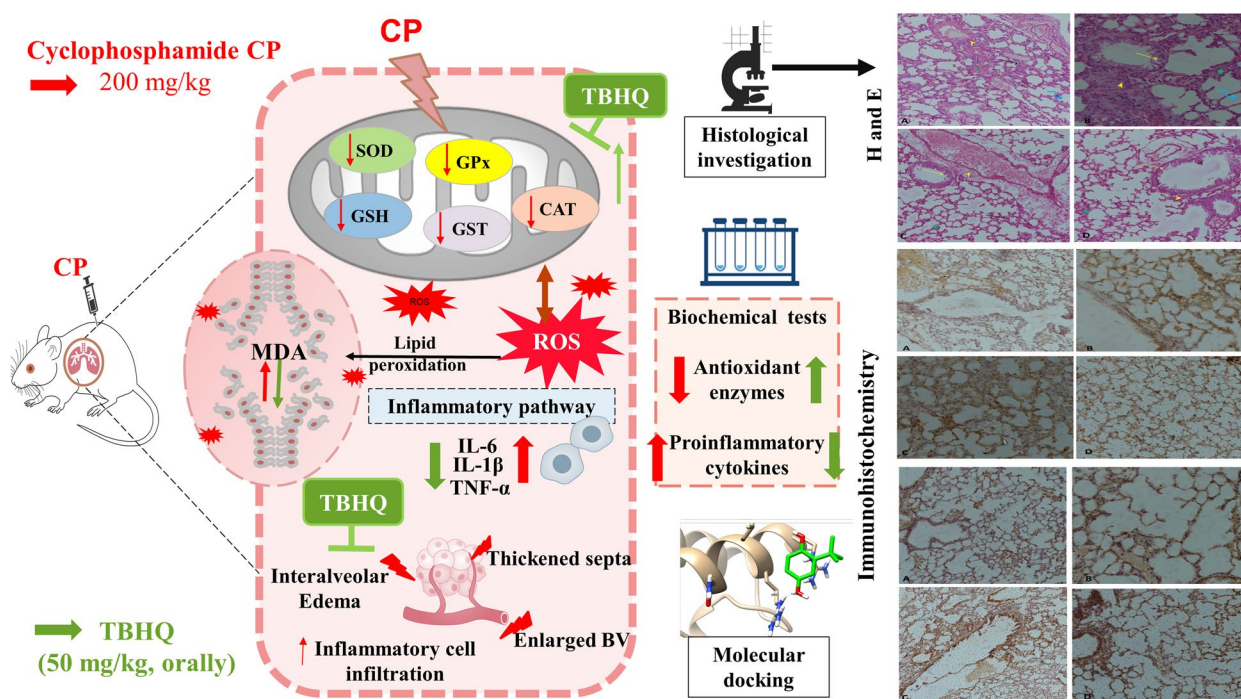
Scheme 2 Summarized experimental design with the results of the study

However, as with any other animal research, there is the limitation of using animals. Both obvious and subtle differences between humans and animals make it difficult to apply data derived from animal studies to human conditions.

Conclusions

In conclusion, the usage of TBHQ showed a protective effect against CP-induced lung toxicity in rats by reducing oxidative stress, apoptosis, inflammation, and histopathological changes. TBHQ augmented antioxidant defenses and decreased proinflammatory levels in the damaged rat's lung induced by CP toxicity. Consequently, TBHQ (with a used dose of 50 mg/kg b.w) may be a useful protective agent during treatment with CP. Further studies are recommended to study the clinical application of TBHQ as a protective agent to overcome anticancer-linked injury.

Abbreviations

AREs	Antioxidant-responsive elements
BSA	Bovine serum albumin
Bcl-2	B cell lymphoma-2
CAT	Catalase
CP	Cyclophosphamide
DAB	Diaminobenzidine tetrahydrochloride
DNA	Deoxyribonucleic acid
DMSO	Dimethyl sulfoxide
GPx	Glutathione peroxidase
GSH	Glutathione
GST	Glutathione S transferase
HRP	Horseradish peroxidase
IL-6	Interleukin-6
IL-1β	Interleukin-1β
MDA	Malondialdehyde
Nrf2	Erythroid 2-related factor 2
ROS/RNS	Reactive oxygen and nitrogen species
RBW	Relative body weight
RLW	Relative lung weight
SOD	Superoxide dismutase
TBHQ	Tert-butylhydroquinone
TNF-α	Tumor necrosis factor-α

Declarations

Ethics approval and consent to participate
The experiment and its procedures complied with the Guide of the Faculty of Science, Suez Canal University research ethics committee of Animal Care and Use (approval no: REC129/2022) and were performed according to the

Ibrahim *et al. Egyptian Journal of Forensic Sciences*   (2024) 14:20

Page 13 of 15

Care and Use of Laboratory Animals published by the US National Institutes of Health (NIH Publication No. 85–23, revised 2011).

Author details
[1]Forensic Medicine and Clinical Toxicology, College of Medicine, Jouf University, Aljouf, Saudi Arabia. [2]Forensic Medicine and Clinical Toxicology Department, Faculty of Medicine, Suez Canal University (SCU), Ismailia 41522, Egypt. [3]Histology Department, College of Medicine, Shaqra University, Shaqra, Saudi Arabia. [4]Histology Department, Faculty of Medicine, Al-Azhar University, Cairo, Egypt. [5]Forensic Medicine and Clinical Toxicology Department, Faculty of Medicine, Al-Azhar University, Damietta, Egypt. [6]Forensic Medicine and Clinical Toxicology Department, College of Medicine, Shaqra University, Shaqra, Saudi Arabia. [7]Pathology Department, College of Medicine, Jouf University, Aljouf, Saudi Arabia. [8]Chemistry Department (Biochemistry Program), Faculty of Science, Suez Canal University, Ismailia 41522, Egypt. [9]Histology Unit, Anatomy Department, College of Medicine, Jouf University, Aljouf, Saudi Arabia. [10]Histology Department, Faculty of Medicine, Al-Azhar University, Assiut, Egypt.

References
Aebi H (1984) [13] Catalase in vitro. In Methods in enzymology (Vol. 105, pp. 121–126). Elsevier. https://doi.org/10.1016/S0076-6879(84)05016-3

Ahmed LA, EL-Maraghy SA, Rizk SM (2015) Role of the KATP channel in the protective effect of nicorandil on cyclophosphamide-induced lung and testicular toxicity in rats. Sci Rep 5(1):Article 1. https://doi.org/10.1038/srep14043

Akhter H, Katre A, Li L, Liu X, Liu R-M (2011) Therapeutic potential and anti-amyloidosis mechanisms of tert-butylhydroquinone for Alzheimer's disease. J Alzheimer's Dis 26(4):767–778. https://doi.org/10.3233/JAD-2011-110512

Aldaba-Muruato LR, Sánchez-Barbosa S, Rodríguez-Purata VH, Cabrera-Cruz G, Rosales-Domínguez E, Martínez-Valentín D, Alarcón-López YA, Aguirre-Vidal P, Hernández-Serda MA, Cárdenas-Granados LA, Vázquez-Valadez VH, Angeles E, Macías-Pérez JR (2024) In vivo and in silico studies of the hepatoprotective activity of tert-butylhydroquinone. Int J Mol Sci 25(1):Article 1. https://doi.org/10.3390/ijms25010475

Alsemeh AE, Abdullah DM (2022) Protective effect of alogliptin against cyclophosphamide-induced lung toxicity in rats: impact on PI3K/Akt/FoxO1 pathway and downstream inflammatory cascades. Cell Tissue Res 388(2):417–438. https://doi.org/10.1007/s00441-022-03593-1

Amiri FT, Hamzeh M, Beklar SY, Hosseinimehr SJ (2018) Anti-apoptotic and antioxidant effect of cerium oxide nanoparticles on cyclophosphamide-induced hepatotoxicity. Erciyes Med J 40(3):148–154. https://doi.org/10.5152/etd.2018.0016

Araghi A, Golshahi H, Baghban F, Tabari MA (2018) Ameliorative action of farnesol on cyclophosphamide induced toxicity in mice. J HerbMed Pharmacol 7(1):37–43. https://doi.org/10.15171/jhp.2018.07

Arnold H, Bourseaux F, Brock N (1958) Chemotherapeutic action of a cyclic nitrogen mustard phosphamide ester (B 518-ASTA) in experimental tumours of the rat. Nature 181(4613):931–931. https://doi.org/10.1038/181931a0

Ashry NA, Gameil NM, Suddek GM (2013) Modulation of cyclophosphamide-induced early lung injury by allicin. Pharm Biol 51(6):806–811

Attia AA, Sorour JM, Mohamed NA, Mansour TT, Al-Eisa RA, El-Shenawy NS (2023) Biochemical, histological, and ultrastructural studies of the protective role of vitamin E on cyclophosphamide-induced cardiotoxicity in male rats. Biomedicines 11(2):Article 2. https://doi.org/10.3390/biomedicines11020390

Ayna A, Özbolat SN, Darendelioglu E (2020) Quercetin, chrysin, caffeic acid and ferulic acid ameliorate cyclophosphamide-induced toxicities in SH-SY5Y cells. Mol Biol Rep 47(11):8535–8543. https://doi.org/10.1007/s11033-020-05896-4

Ayza MA, Zewdie KA, Yigzaw EF, Ayele SG, Tesfaye BA, Tafere GG, Abrha MG (2022) Potential protective effects of antioxidants against cyclophosphamide-induced nephrotoxicity. Int J Nephrol 2022:e5096825. https://doi.org/10.1155/2022/5096825

Badawi MS (2022) The protective effect of β-cryptoxanthin against cyclophosphamide-induced lung injury in adult male albino rats. Bull Nat l Res Centre 46(1):106. https://doi.org/10.1186/s42269-022-00792-2

Boss AP, Freeborn RA, Duriancik DM, Kennedy RC, Gardner EM, Rockwell CE (2018) The Nrf2 activator tBHQ inhibits the activation of primary murine natural killer cells. Food Chem Toxicol 121:231–236. https://doi.org/10.1016/j.fct.2018.08.067

Chabra A, Shokrzadeh M, Naghshvar F, Salehi F, Ahmadi A (2014) Melatonin ameliorates oxidative stress and reproductive toxicity induced by cyclophosphamide in male mice. Hum Exp Toxicol 33(2):185–195. https://doi.org/10.1177/0960327113489052

Conte P, Ascierto PA, Patelli G, Danesi R, Vanzulli A, Sandomenico F, Tarsia P, Cattelan A, Comes A, De Laurentiis M, Falcone A, Regge D, Richeldi L, Siena S (2022) Drug-induced interstitial lung disease during cancer therapies: Expert opinion on diagnosis and treatment. ESMO Open 7(2):100404. https://doi.org/10.1016/j.esmoop.2022.100404

Dai S, Wang C, Feng L, Zhang C, Zhang W, He Y, Zhou X, Xia X, Chen B, Song W (2022) Protective activity of tert-butylhydroquinone against oxidative stress and apoptosis induced by glutamate agonizts in R28 cells and mice retina. Biomed Pharmacother 152:113117. https://doi.org/10.1016/j.biopha.2022.113117

de Jonge ME, Huitema ADR, Rodenhuis S, Beijnen JH (2005) Clinical pharmacokinetics of cyclophosphamide. Clin Pharmacokinet 44(11):1135–1164. https://doi.org/10.2165/00003088-200544110-00003

Deng S, Wu D, Li L, Li J, Xu Y (2021) TBHQ attenuates ferroptosis against 5-fluorouracil-induced intestinal epithelial cell injury and intestinal mucositis via activation of Nrf2. Cell Mol Biol Lett 26(1):48. https://doi.org/10.1186/s11658-021-00294-5

Devi HP, Mazumder PB (2016) Methanolic extract of curcuma caesia Roxb. prevents the toxicity caused by cyclophosphamide to bone marrow cells, liver and kidney of mice. Pharmacognosy Res 8(1):43–49. https://doi.org/10.4103/0974-8490.171106

Duan X, Li J, Li W, Xing X, Zhang Y, Li W, Zhao L, Sun G, Gao X, Li B (2016) Antioxidant tert-butylhydroquinone ameliorates arsenic-induced intracellular damages and apoptosis through induction of Nrf2-dependent antioxidant responses as well as stabilization of anti-apoptotic factor Bcl-2 in human keratinocytes. Free Radical Biol Med 94:74–87. https://doi.org/10.1016/j.freeradbiomed.2016.02.009

Elgohary R, Salama A, Omara EA (2023) Protective effects of Cannabis sativa on chemotherapy-induced nausea in a rat: involvement of CB1 receptors. Fundam Clin Pharmacol 37(1):137–146. https://doi.org/10.1111/fcp.12821

El-Kashef DH (2018) Role of venlafaxine in prevention of cyclophosphamide-induced lung toxicity and airway hyperactivity in rats. Environ Toxicol Pharmacol 58:70–76

El-Naggar SA, Alm-Eldeen AA, Germoush MO, El-Boray KF, Elgebaly HA (2015) Ameliorative effect of propolis against cyclophosphamide-induced toxicity in mice. Pharm Biol 53(2):235–241. https://doi.org/10.3109/13880209.2014.914230

Emadi A, Jones RJ, Brodsky RA (2009) Cyclophosphamide and cancer: golden anniversary. Nat Rev Clin Oncol 6(11):Article 11. https://doi.org/10.1038/nrclinonc.2009.146

Ghosh P, Bhattacharjee A, Basu A, Singha Roy S, Bhattacharya S (2015) Attenuation of cyclophosphamide-induced pulmonary toxicity in Swiss albino mice by naphthalimide-based organoselenium compound 2-(5-selenocyanatopentyl)-benzo [de] isoquinoline 1, 3-dione. Pharm Biol 53(4):524–532

Habibi E, Shokrzadeh M, Ahmadi A, Chabra A, Naghshvar F, Haghi-Aminjan H, Salehi F (2020) Pulmonoprotective action of Zataria multiflora ethanolic extract on cyclophosphamide-induced oxidative lung toxicity in mice. Chin J Integr Med 26(10):754–761. https://doi.org/10.1007/s11655-018-2984-4

Ibrahim *et al. Egyptian Journal of Forensic Sciences*   (2024) 14:20

Page 14 of 15

Habig, W. H., & Jakoby, W. B. (1981). [51] Assays for differentiation of glutathione S-Transferases. In Methods in Enzymology (Vol. 77, pp. 398–405). Academic Press. https://doi.org/10.1016/S0076-6879(81)77053-8

Ibrahim HM, Mohammed-Geba K, Tawfic AA, El-Magd MA (2019) Camel milk exosomes modulate cyclophosphamide-induced oxidative stress and immuno-toxicity in rats. Food Funct 10(11):7523–7532. https://doi.org/10.1039/c9fo01914f

Imran M, Lim IK (2013) Regulation of Btg2/TIS21/PC3 expression via reactive oxygen species–protein kinase C-NFκB pathway under stress conditions. Cell Signal 25(12):2400–2412. https://doi.org/10.1016/j.cellsig.2013.07.015

Jiang W, Liu J, Li P, Lu Q, Pei X, Sun Y, Wang G, Hao K (2017) Magnesium isoglycyrrhizinate shows hepatoprotective effects in a cyclophosphamide-induced model of hepatic injury. Oncotarget 8(20):33252. https://doi.org/10.18632/oncotarget.16629

Kachel D, Martin W (1994) Cyclophosphamide-induced lung toxicity: Mechanism of endothelial cell injury. J Pharmacol Exp Ther 268(1):42–46

Kamiya A, Machida T, Hirano M, Machida M, Shiga S, Hamaue N, Hirafuji M, Iizuka K (2021) Administration of cyclophosphamide to rats induces pica and potentiates 5-hydroxytryptamine synthesis in the intestine without causing severe intestinal injury. J Pharmacol Sci 147(3):251–259. https://doi.org/10.1016/j.jphs.2021.07.007

Kanno TYN, Sensiate LA, de Paula NA, Salles MJS (2009) Toxic effects of different doses of cyclophosphamide on the reproductive parameters of male mice. Braz J Pharm Sci 45:313–319. https://doi.org/10.1590/S1984-82502009000200017

Kensler TW, Wakabayashi N, Biswal S (2007) Cell survival responses to environmental stresses via the Keap1-Nrf2-ARE pathway. Annu Rev Pharmacol Toxicol 47(1):89–116. https://doi.org/10.1146/annurev.pharmtox.46.120604.141046

Khezerlou A, Akhlaghi AP, Alizadeh AM, Dehghan P, Maleki P (2022) Alarming impact of the excessive use of tert-butylhydroquinone in food products: a narrative review. Toxicol Rep 9:1066–1075. https://doi.org/10.1016/j.toxrep.2022.04.027

Kim J, Chan JJ (2017) Cyclophosphamide in dermatology. Australas J Dermatol 58(1):5–17. https://doi.org/10.1111/ajd.12406

Koh K, Cha Y, Kim S, Kim J (2009) TBHQ inhibits LPS-induced microglial activation via Nrf2-mediated suppression of p38 phosphorylation. Biochem Biophys Res Commun 380(3):449–453. https://doi.org/10.1016/j.bbrc.2009.01.082

Lawrence RA, Burk RF (1978) Species, tissue and subcellular distribution of non se-dependent glutathione peroxidase activity. J Nutr 108(2):211–215. https://doi.org/10.1093/jn/108.2.211

Li Y, Cao Y, Wang F, Pu S, Zhang Y, Li C (2014) Tert-butylhydroquinone attenuates scrotal heat-induced damage by regulating Nrf2-antioxidant system in the mouse testis. Gen Comp Endocrinol 208:12–20. https://doi.org/10.1016/j.ygcen.2014.09.007

Li R, Zhang P, Li C, Yang W, Yin Y, Tao K (2020) Tert-butylhydroquinone mitigates carbon tetrachloride induced hepatic injury in mice. Int J Med Sci 17(14):2095–2103. https://doi.org/10.7150/ijms.45842

Liu T, Li C, Chen H, Liu J, Zhong L, Tang M, Wang W, Huang J, Jiang X (2022) TBHQ attenuates podocyte injury in diabetic nephropathy by inhibiting NADPH oxidase-derived ROS generation via the Nrf2/HO-1 signalling pathway. Heliyon 8(9):e10515

López PL, Juncos NS, Grosso NR, Olmedo RH (2022) Minthostachys mollis essential oil and its combination with tert-butylhydroquinone for control of lipid oxidation. Eur J Lipid Sci Technol 124(11):2200081. https://doi.org/10.1002/ejlt.202200081

Meng X, Zhang C, Guo Y, Han Y, Wang C, Chu H, Kong L, Ma H (2020) TBHQ attenuates neurotoxicity induced by methamphetamine in the VTA through the Nrf2/HO-1 and PI3K/AKT signaling pathways. Oxid Med Cell Longev 2020:8787156. https://doi.org/10.1155/2020/8787156

Mills KA, Chess-Williams R, McDermott C (2019) Novel insights into the mechanism of cyclophosphamide-induced bladder toxicity: chloroacetaldehyde's contribution to urothelial dysfunction in vitro. Arch Toxicol 93(11):3291–3303. https://doi.org/10.1007/s00204-019-02589-1

Möller B, Villiger PM (2006) Inhibition of IL-1, IL-6, and TNF-α in immune-mediated inflammatory diseases. Springer Semin Immunopathol 27(4):391–408. https://doi.org/10.1007/s00281-006-0012-9

Mombeini MA, Kalantar H, Sadeghi E, Goudarzi M, Khalili H, Kalantar M (2022) Protective effects of berberine as a natural antioxidant and anti-inflammatory agent against nephrotoxicity induced by cyclophosphamide in

mice. Naunyn-Schmiedeberg's Arch Pharmacol 395(2):187–194. https://doi.org/10.1007/s00210-021-02182-3

Mythili Y, Sudharsan PT, Selvakumar E, Varalakshmi P (2004) Protective effect of dl-α-lipoic acid on cyclophosphamide induced oxidative cardiac injury. Chem Biol Interact 151(1):13–19. https://doi.org/10.1016/j.cbi.2004.10.004

Nafie MS, Tantawy MA, Elmgeed GA (2019) Screening of different drug design tools to predict the mode of action of steroidal derivatives as anti-cancer agents. Steroids 152:108485. https://doi.org/10.1016/j.steroids.2019.108485

Nna VU, Ujah GA, Suleiman JB, Mohamed M, Nwokocha C, Akpan TJ, Ekuma HC, Fubara VV, Kekung-Asu CB, Osim EE (2020) Tert-butylhydroquinone preserve testicular steroidogenesis and spermatogenesis in cisplatin-intoxicated rats by targeting oxidative stress, inflammation and apoptosis. Toxicology 441:152528. https://doi.org/10.1016/j.tox.2020.152528

Olama NK, Taha M, Rady HY (2018) The potential protective role of coenzyme q10 on the cyclophosphamide-induced lung toxicity in adult male albino rats: A histological and ultrastructural study. Int J Sci Rep 4(9):225. https://doi.org/10.18203/issn.2454-2156.intjscirep20183618

Omole JG, Ayoka OA, Alabi QK, Adefisayo MA, Asafa MA, Olubunmi BO, Fadeyi BA (2018) Protective effect of kolaviron on cyclophosphamide-induced cardiac toxicity in rats. J Evid Based Integr Med 23:2156587218757649

Patra K, Bose S, Sarkar S, Rakshit J, Jana S, Mukherjee A, Roy A, Mandal DP, Bhattacharjee S (2012) Amelioration of cyclophosphamide induced myelosuppression and oxidative stress by cinnamic acid. Chem Biol Interact 195(3):231–239. https://doi.org/10.1016/j.cbi.2012.01.001

Pérez-Rojas JM, Guerrero-Beltrán CE, Cruz C, Sánchez-González DJ, Martínez-Martínez CM, Pedraza-Chaverri J (2011) Preventive effect of tert-butylhydroquinone on cisplatin-induced nephrotoxicity in rats. Food Chem Toxicol 49(10):2631–2637. https://doi.org/10.1016/j.fct.2011.07.008

Placer ZA, Cushman LL, Johnson BC (1966) Estimation of product of lipid peroxidation (malonyl dialdehyde) in biochemical systems. Anal Biochem 16(2):359–364

PubChem. (n.d.). PubChem. Retrieved 7 March 2023, from https://pubchem.ncbi.nlm.nih.gov/

Raeeszadeh M, Saleh Hosseini SM, Amiri AA (2022) Impact of co-administration of N-acetylcysteine and vitamin E on cyclophosphamide-induced ovarian toxicity in female rats. J Toxicol 2022:e9073405. https://doi.org/10.1155/2022/9073405

Saghir SAM, Alharbi SA, Al-Garadi MA, Al-Gabri N, Rady HY, Olama NK, Abdulghani MAM, Al Hroob AM, Almaiman AA, Bin-Jumah M, Mahmoud AM, Taha M (2020) Curcumin prevents cyclophosphamide-induced lung injury in rats by suppressing oxidative stress and apoptosis. Processes 8(2):Article 2. https://doi.org/10.3390/pr8020127

Said E, Elkashef WF, Abdelaziz RR (2016) Tranilast ameliorates cyclophosphamide-induced lung injury and nephrotoxicity. Can J Physiol Pharmacol 94(4):347–358. https://doi.org/10.1139/cjpp-2015-0070

Salama RM, Nasr MM, Abdelhakeem JI, Roshdy OK, ElGamal MA (2022) Alogliptin attenuates cyclophosphamide-induced nephrotoxicity: a novel therapeutic approach through modulating MAP3K/JNK/SMAD3 signaling cascade. Drug Chem Toxicol 45(3):1254–1263. https://doi.org/10.1080/01480545.2020.1814319

Sargazi S, Moghadam Jafari A & Heidarpour M (2015) Tert-butylhydroquinone (TBHQ) improves antioxidant status in rat tissues following chronic diazinon intoxication. Iran J Vet Sci Technol 6(February 2018). https://doi.org/10.22067/veterinary.v6i2.39503

Saykally JN, Rachmany L, Hatic H, Shaer A, Rubovitch V, Pick CG, Citron BA (2012) The nuclear factor erythroid 2-like 2 activator, tert-butylhydroquinone, improves cognitive performance in mice after mild traumatic brain injury. Neuroscience 223:305–314. https://doi.org/10.1016/j.neuroscience.2012.07.070

Sedlak J, Lindsay RH (1968) Estimation of total, protein-bound, and nonprotein sulfhydryl groups in tissue with Ellman's reagent. Anal Biochem 25:192–205

Şengül E, Gelen V, Gedikli S, Özkanlar S, Gür C, Çelebi F, Çınar A (2017) The protective effect of quercetin on cyclophosphamide-Induced lung toxicity in rats. Biomed Pharmacother 92:303–307

Shokrzadeh M, Chabra A, Naghshvar F, Ahmadi A, Jafarinejhad M, Hasani-Nourian Y (2015) Protective effects of melatonin against cyclophosphamide-induced oxidative lung toxicity in mice. Drug Research 65(6):281–286. https://doi.org/10.1055/s-0034-1371801

SPSS, I. (2015). IBM SPSS statistics for windows, version 23.0. Armonk: IBM Corp.

Sun Y, Oberley LW, Li Y (1988) A simple method for clinical assay of superoxide dismutase. Clin Chem 34(3):497–500. https://doi.org/10.1093/clinchem/34.3.497

Sun Y, Ito S, Nishio N, Tanaka Y, Chen N, Isobe K (2014) Acrolein induced both pulmonary inflammation and the death of lung epithelial cells. Toxicol Lett 229(2):384–392. https://doi.org/10.1016/j.toxlet.2014.06.021

Ujah GA, Nna VU, Suleiman JB, Eleazu C, Nwokocha C, Rebene JA, Imowo MU, Obi EO, Amachree C, Udechukwu EC, Mohamed M (2021) Tert-butylhydroquinone attenuates doxorubicin-induced dysregulation of testicular cytoprotective and steroidogenic genes, and improves spermatogenesis in rats. Sci Rep 11(1):Article 1. https://doi.org/10.1038/s41598-021-85026-7

Vahid B, Marik PE (2008) Pulmonary complications of novel antineoplastic agents for solid tumors. Chest 133(2):528–538. https://doi.org/10.1378/chest.07-0851

Veskemaa L, Graw JA, Pickerodt PA, Taher M, Boemke W, González-López A, Francis RCE (2021) Tert-butylhydroquinone augments Nrf2-dependent resilience against oxidative stress and improves survival of ventilator-induced lung injury in mice. Am J Physiol Lung Cell Mol Physiol 320(1):L17–L28. https://doi.org/10.1152/ajplung.00131.2020

Voelcker G (2020) The mechanism of action of cyclophosphamide and its consequences for the development of a new generation of oxazaphosphorine cytostatics. Scientia Pharmaceutica 88(4):4. https://doi.org/10.3390/scipharm88040042

Wu J, Cheng M, Liu Q, Yang J, Wu S, Lu X, Jin C, Ma H, Cai Y (2015) Protective role of tert-butylhydroquinone against sodium fluoride-induced oxidative stress and apoptosis in PC12 cells. Cell Mol Neurobiol 35(7):1017–1025. https://doi.org/10.1007/s10571-015-0196-4

Xiong R, Wu Q, Bryant M, Rosenfeldt H, Healy S, Cao X (2021) In vitro dosimetry analyses for acrolein exposure in normal human lung epithelial cells and human lung cancer cells. Environ Toxicol Pharmacol 83:103576. https://doi.org/10.1016/j.etap.2020.103576

Xu W, Li F, Xu Z, Sun B, Cao J, Liu Y (2017) Tert-butylhydroquinone protects PC12 cells against ferrous sulfate-induced oxidative and inflammatory injury via the Nrf2/ARE pathway. Chem Biol Interact 273:28–36

Yang S, Shi W, Liu Q, Song Y, Fang J (2023) Nrf2 enhances the therapeutic efficiency of adipose-derived stem cells in the treatment of neurogenic erectile dysfunction in a rat model. Basic Clin Androl 33(1):39. https://doi.org/10.1186/s12610-023-00214-x

Yuan D, Wang H, He H, Jia L, He Y, Wang T, Zeng X, Li Y, Li S, Zhang C (2014) Protective effects of total flavonoids from epimedium on the male mouse reproductive system against cyclophosphamide-induced oxidative injury by up-regulating the expressions of SOD3 and GPX1. Phytother Res 28(1):88–97. https://doi.org/10.1002/ptr.4956

Zeng X-P, Li X-J, Zhang Q-Y, Liu Q-W, Li L, Xiong Y, He C-X, Wang Y-F, Ye Q-F (2017) Tert-butylhydroquinone protects liver against ischemia/reperfusion injury in rats through Nrf2-activating anti-oxidative activity. Transpl Proc 49(2):366–372. https://doi.org/10.1016/j.transproceed.2016.12.008

Zhang J, Tucker LD, DongYan, Lu Y, Yang L, Wu C, Li Y, Zhang Q (2018) Tert-butylhydroquinone post-treatment attenuates neonatal hypoxic-ischemic brain damage in rats. Neurochem Int 116:1–12. https://doi.org/10.1016/j.neuint.2018.03.004

Zhang Z-W, Liang J, Yan J-X, Ye Y-C, Wang J-J, Chen C, Sun H-T, Chen F, Tu Y, Li X-H (2020) TBHQ improved neurological recovery after traumatic brain injury by inhibiting the overactivation of astrocytes. Brain Res 1739:146818. https://doi.org/10.1016/j.brainres.2020.146818

Zhang H, Li J, Xiang X, Zhou B, Zhao C, Wei Q, Sun Y, Chen J, Lai B, Luo Z (2021) Tert-butylhydroquinone attenuates osteoarthritis by protecting chondrocytes and inhibiting macrophage polarization. Bone Joint Res 10(11):704–713

Zhao YL, Zhao W, Liu M, Liu L, Wang Y (2020) TBHQ-overview of multiple mechanisms against oxidative stress for attenuating methamphetamine-induced neurotoxicity. Oxid Med Cell Longev 2020(2020):8874304

Zhu T, Zhu C-N, Huang N, Yu X, Wan G, Wang S, Song P, Xu J, Li P, Yin Y (2022) Tert-Butylhydroquinone alleviates insulin resistance and liver steatosis in diabetes. Indian J Pharmacol 54(2):118–125. https://doi.org/10.4103/ijp.ijp_440_21

Publisher's Note